Atmospheric IR Transmittance Statistics in Arid Climates Based upon Synoptic Data from Selected Middle East Weather Stations

D. H. Höhn, W. Jessen, D. Clement

Forschungsgesellschaft fur Angewandte Naturwissenschaften
Forschungsinstitut für Optik (FGAN-FfO)
Dok. Nr. 1996/57
Schloss Kressbach
D-72072 Tubingen, Germany

1. General

Operations in desert environments may be influenced by effects not found under climatic conditions of middle latitudes. Apart from the different general climatic situations also other effects typical for desert regions will affect systems operation, e. g. through blowing dust and sand by reducing atmospheric transmittance of electro-magnetic radiation. This can cause severe problems in system operation and even prevent it.

This study analyzes synoptic weather data from nine Middle East meteorological stations. Furthermore, to characterize ir propagation conditions the atmospheric transmittance was derived from the meteorological data. The resulting statistics are presented and analyzed.

The stations cover a wide geographical range from the northern Middle East states to the southern part of the Saudi-Arabian peninsula. It is assumed that this choice will describe typical climatic areas of interest.

2. Origin and Scope of Source Data

Synoptic weather data from the Middle East desert regions formed the basis for the following climatological survey. They are available to FGAN-FfO through the Global Telecommunication Service (GTS) of the World Meteorological Organization (WMO). The national data bank of GTS data is held by the German Weather Service, Seewetteramt Hamburg (SWA), which distributes the data.

The data covers the complete set of meteorological parameters as collected world-wide at fixed synoptic hours of observation. A total period of one year of observations has been evaluated for nine meteorological stations as listed below in Table 1.

block-nr.	station-nr.	period	longitude degr. E	latitude degr. N	name	(country)
40	072	1985	40,9	34.4	Abu-Kamal	(s)
40	250	1985	38.2	32.5	H4	(J)
40	310	1985	35.8	30.2	Ma'an	(J)
40	340	1985	35.0	29.6	Aqaba	(J)
40	356	1985	38.7	31.7	Al-Turayf	(A)
40	394	1985	41.7	27.4	Hail	(A)
41	024	1985	39,2	21.7	Jiddah	(A)
41	062	1985	45,6	20,5	Sulayel	(A)
41	136	1985	47.2	17.5	Sharurah	(A)

Table 1: Nine selected Middle East meteorological stations with geographical location and time period covered. The first two columns indicate the international block number and the station number for identification.

(S: Syria, J: Jordan, A: Saudi-Arabia)

Fig. 1 presents a map to illustrate the geographical positions of each station. Obviously seven of these stations are lying in desert or desert-like territory, whereas two of them (Aqaba and Jiddah) have a coastal environment. Note that the desert stations partly have a considerable large altitude above sea level.

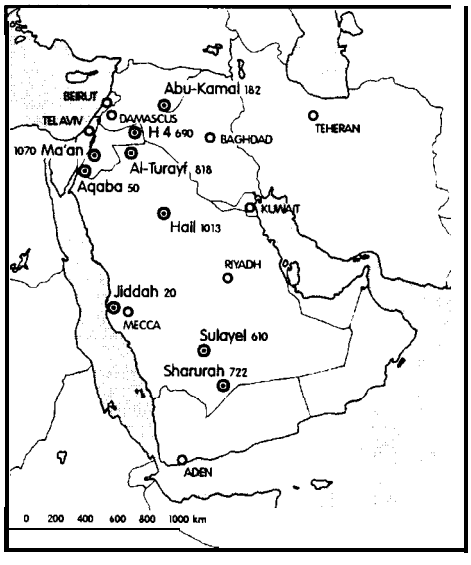

Fig. 1: Geographical location of nine selected Middle East meteorological stations. Numbers indicate altitude in m above sea level.

The data from the GTS through the SWA is distributed in a coded form (SWASYNOP) similar to the international weather code of the WMO. It has to be decoded before use. Furthermore it is generally uncorrected and therefore requires a thorough inspection and validation. Both procedures have been applied in the FGAN-FfO to the data set described above. The Saudi-Arabian observations are nearly complete. The other stations (Syria and Jordan) show larger gaps, preferably during night hours. Therefore for detailed studies only the Saudi-Arabian stations were considered.

3. Data Structure and Evaluation

All available data were stored on one file for each station in chronological order. The parameters contained in each file are listed in Table 2.

General Data and File Identification
Julian date, block-nr., station-nr., altitude a.s.l., longitude, latitude, date, time (UTC)
Observed Parameter
Present weather, incl. cloud cover
Pressure at station, pressure reduced to sea level
Visual range, wind speed and wind direction
Temperature, dew point temperature
Amount of precipitation since last observation
Derived Quantities
Relative humidity
Absolute humidity
IR transmittance (3 -5 pm, 8-13 μm) over 1 km range: molecular, aerosol, total

Table 2: Quantities contained in each record of the data file.

As mentioned above one file for each meteorological station was created. They can serve as a data base for further analyses. To complement the original data some derived quantities have been added as listed in Table 2.

The transmittances were calculated (for 1 km horizontal range) after SYTRAN [1] which is a short version of LOWTRAN 7 [2], assuming a transmissometer source temperature of 650 “C and standardized system response functions for both atmospheric window regions (3 - 5 μm and 8-13 pm).

The molecular contribution to atmospheric transmittance is fairly well known from LOWTRAN. The calculation of the transmittance contribution due to atmospheric aerosols requires the assumption of an aerosol model as long as no further information - for example transmission measurements - is available. The following study makes use of the LOWTRAN 7 Desert Aerosol Model throughout. For the coastal stations, which have been included for comparisons, this assumption may not be justified. Therefore the aerosol transmittances at these locations must be considered with care. This Desert Aerosol Model is described in detail in [3]. In its original form it describes the atmospheric aerosol mass loading as a function of wind speed only. It represents an average of many findings and is not more than a generic rather than a specific model. Other than in [3] it is possible to enter in LOWTRAN 7 an observed visual range as an input parameter for scaling the resulting aerosol transmittance according to visibility.

The data evaluation has been performed in several steps. In a first step time series of a number of meteorological parameters were plotted to get an overview of occurring annual and diurnal variations. Also for the derived quantities time series plots are available. Examples will be shown below. In a second step statistical evaluations were performed in the form of cumulative frequency distributions of meteorological and other, derived parameters over the whole year. The third step dealt with the annual variability of the cumulative frequency distribution of trans-

mittance. Some selected results also on this topic are given below. An estimate of thermal imagers ranges statistics is given in the last section

4. **Data Presentation and Statistical Results**

Selected examples of the data evaluation and general statistical results are summarized in the following chapter.

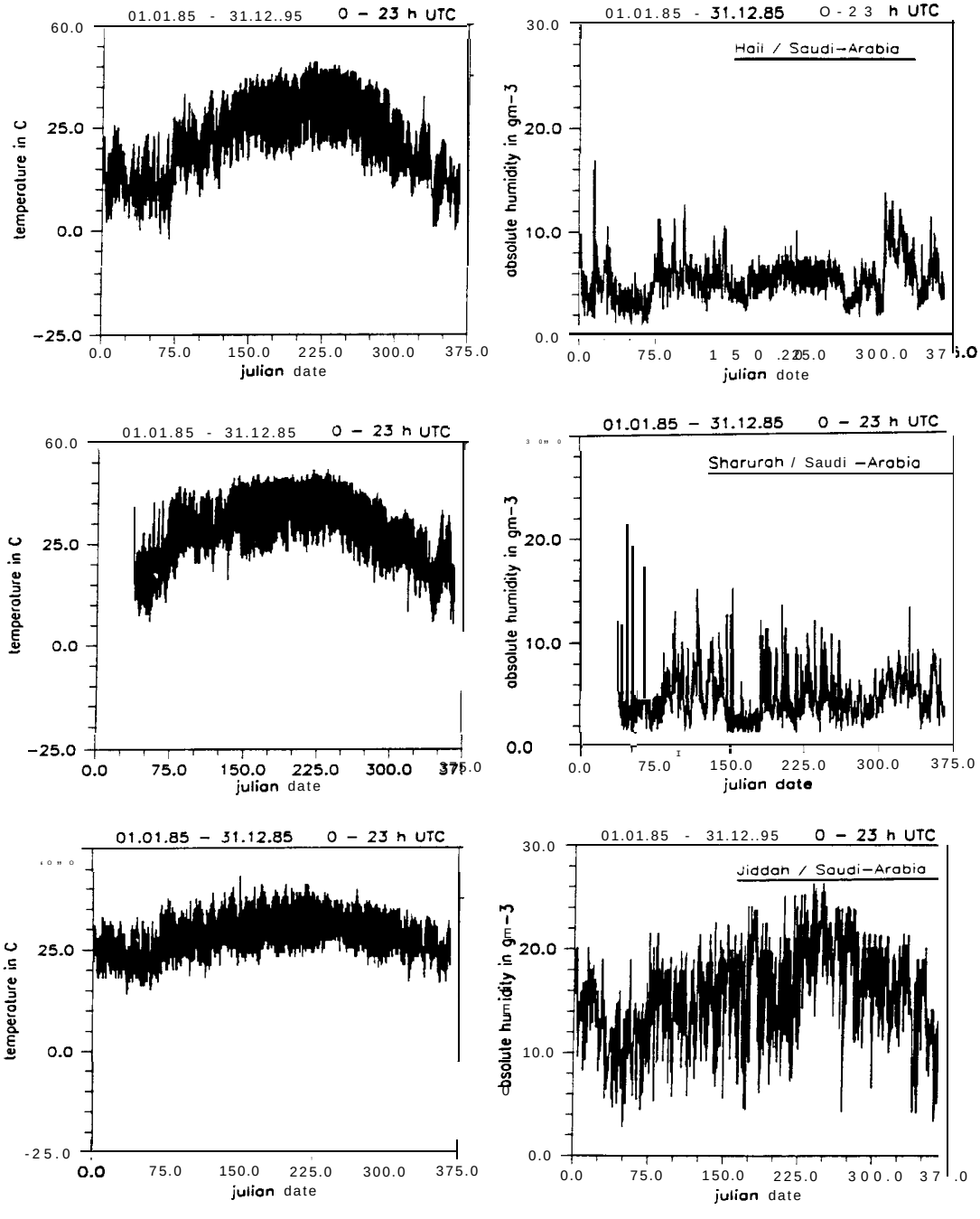

Fig. 2: Temperature (left) and absolute humidity (right) as a function of the Julian date at stations Hail, Sharurah, and Jiddah (Saudia-Arabia).

4.1 Selected Time Series of General Meteorological Data

In Fig. 2 time series over one year of atmospheric temperature and absolute humidity at three of the Middle East stations are presented.

The annual variation of temperature can reach an amplitude of nearly 40 “C at least in typical desert locations as shown in Fig. 2. In contrast the station Jiddah shows a more moderate amplitude of less than 20 °C due to its coastal environment. However, in both cases considerable diurnal variations of nearly 20 “C are observed. It should be mentioned that temperature in the desert even can reach the freezing point during nights of extreme radiative cooling. This is especially the case at higher altitudes, e. g. at Hail (see Figs. 1 and 2).

The absolute humidity can also vary extremely rapidly and reaches maximum values in Jiddah with extreme humidities in late summer of 20-25 gi^{n-3}. All other stations examined in this study never reach these extreme absolute humidities, which obviously is related to the coastal position. Only Aqaba as a station near coast has comparable humidities. Cumulative probabilities of visual range V_N are shown in Fig. 3. At the stations considered, V_N rarely exceeds 15 km. This is a clear contradiction to the prediction contained in the original Desert Aerosol Model [3]. There a value $V_N \approx 80$ km is quoted for calm conditions. Therefore simultaneous measurements of meteorological, ir and aerosol conditions at desert locations seem extremely necessary. They are currently under preparation by the FGAN-FfO. Furthermore, the results seem to indicate a need for more sophisticated desert type aerosol models. The discrepancy may result from visibility estimation conventions or even from observational errors or inadequate positioning of visibility marks near the observation site.

4.2 Cumulative Probabilities of IR Transmittances

The calculated transmittances at the nine Middle East meteorological stations have been evaluated in the form of cumulative transmittance curves. In Fig. 4 some exemplary results are presented for the Middle East desert region (stations Hail, Sulayel and Sharurah) and the coastal station Jiddah. As stated earlier, the LOWTRAN 7 Desert Aerosol Model was applied throughout. Fig. 4 shows the molecular, aerosol, and total transmittance, respectively, for both atmospheric window regions (3 -5 µm left, and 8-13 µm right). The molecular contribution is strongly related to the atmospheric water content, which assumes excessive values at the coastal station of Jiddah. Consequently the cumulative curve of Jiddah deviates strongly from those of all other stations. (The water content at Jiddah has already been shown in Fig. 2). In general the transmittance (over 1 km range as shown here) at 8-13 µm is approximately 10-15 % larger in comparison with the 3-5 µm region. For Jiddah, a strong broadening of the molecular transmittance distribution is observed when changing from the 3-5 µm region to 8 -13 pm. This effect must be attributed to the weaker water vapor dependence of absorption in the 3-5 µm region in comparison to the 8-13 µm region, which becomes even more effective at extreme high water contents (above 15 gm^{-3}) as occurring at Jiddah.

The aerosol transmittances are quite similar at all stations and for both regions as can to be seen from Fig. 4 (middle). The partly stepped curves reflect the wind and mainly the visibility statistics, which are often given by rough step functions due to human eye observations or instrumental readings. Fig. 4 (bottom) shows the total transmittance statistics. As aerosol transmittance usually is relatively high mainly the molecular contribution determines the total trans-

mittance and the form of the cumulative curves. But still further analyses based on relevant measurements will have to take into account risibilities exceeding 15 km and should be based on experimentally proven aerosol models.

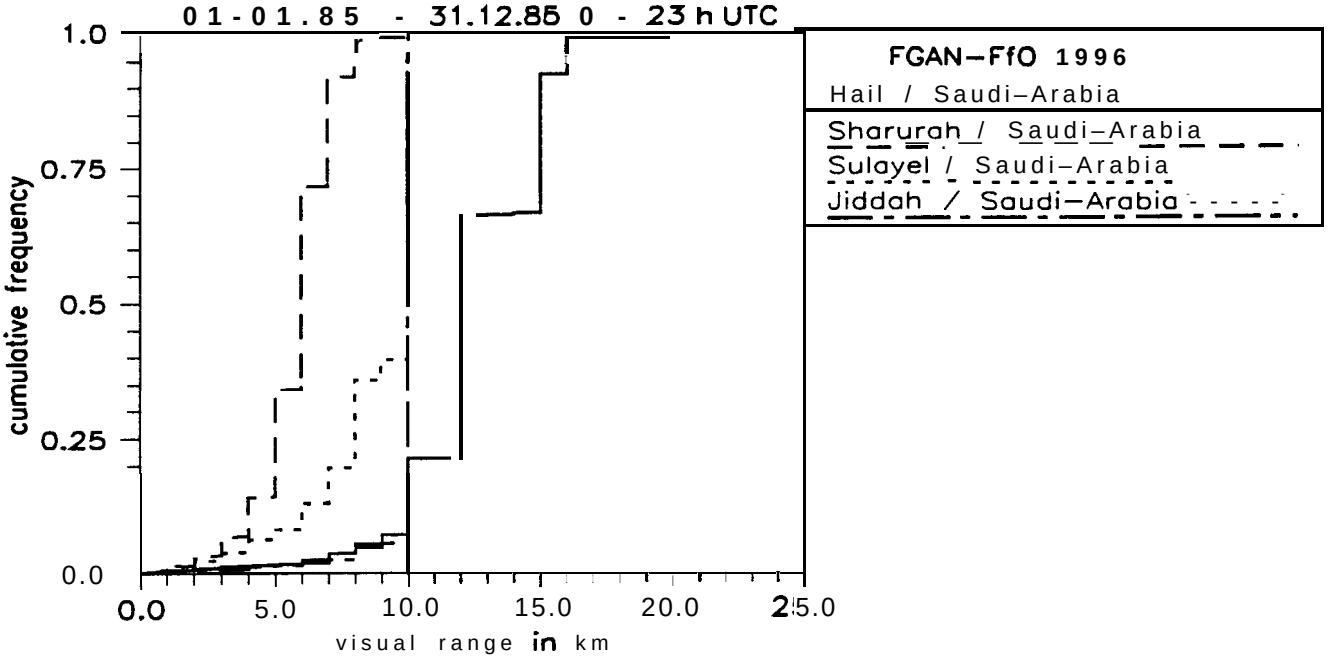

Fig. 3: **Cumulative probabilities of visual range based on 1 year of observations (1985) at the desert stations Hail. Sulayel, and Sharurah, and the coastal station Jiddah.**

(Values exceeding 15 km seem not to occur due to observation / documentation conventions used)

4.3 Annual Variability of IR Propagation Conditions

So far only annual statistics data have been presented. Fig. 5 illustrates the seasonal variability of seven n-percentiles (n = 5, 10, 25, 50, 75, 90, 95) of the total transmittances (3 -5 µm and 8-13 pm) for the stations Jiddah and Sulayel which seem to be representative for a coastal and a central desert station, respectively.

A relatively broad distribution in the 8-13 µm region can be observed in Jiddah, which shrinks to a nearly constant value over the whole year in the 3-5 µm region, caused by the weaker dependence against water content variations mentioned under 4.2. The annual variations are comparatively small, also in the 8-13 µm region, and probably also influenced by local circulation systems which cannot be analyzed in detail without further information about the different locations of the meteorological stations involved in this study.

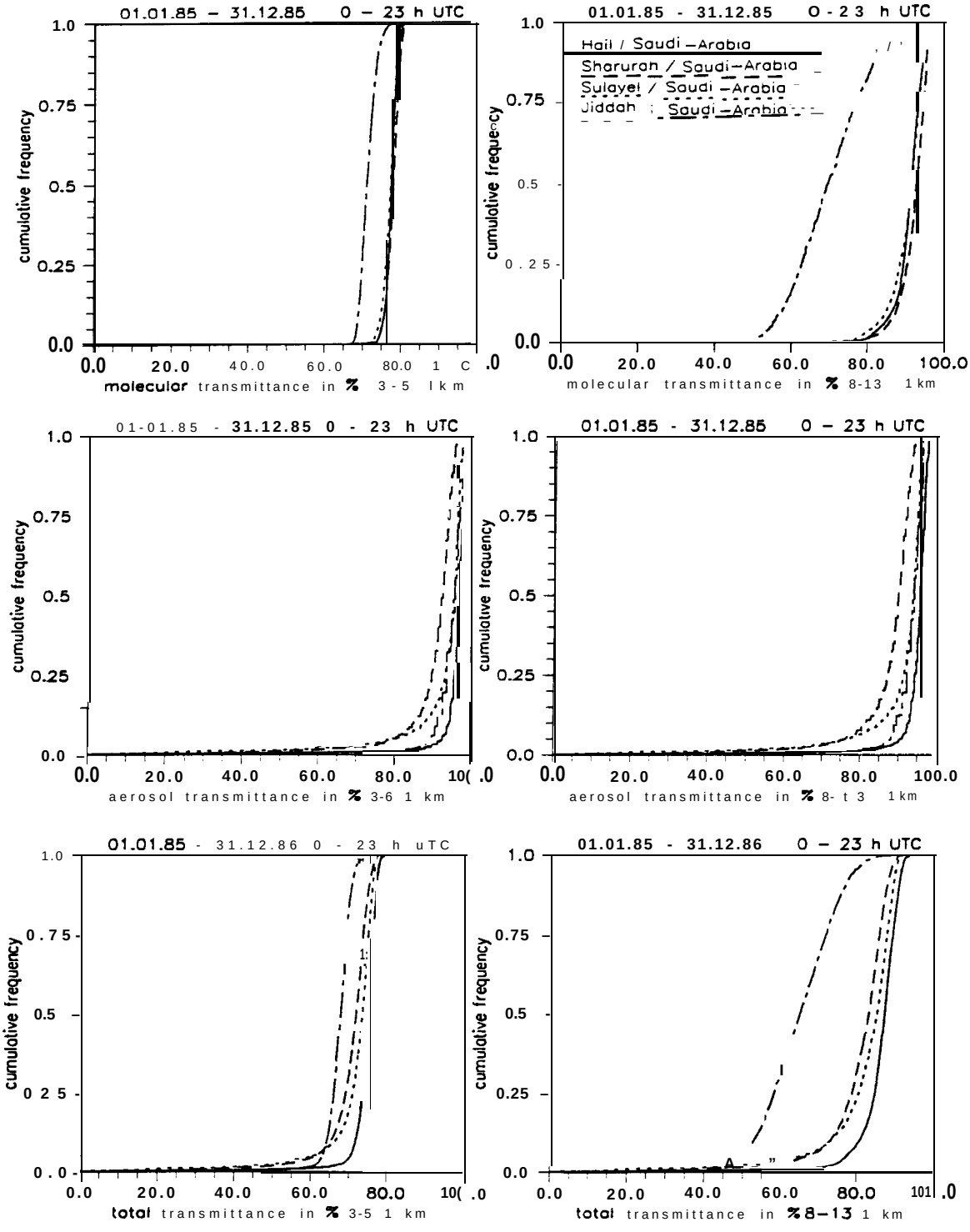

Fig. 4: Cumulative frequencies of molecular (top), aerosol (middle) and total (bottom) ir transmittances over 1 km range for stations Hail, Sharurah, Sulayel and Jiddah: wavelength regions 3- 5pm (left) and 8 -13pm (right).

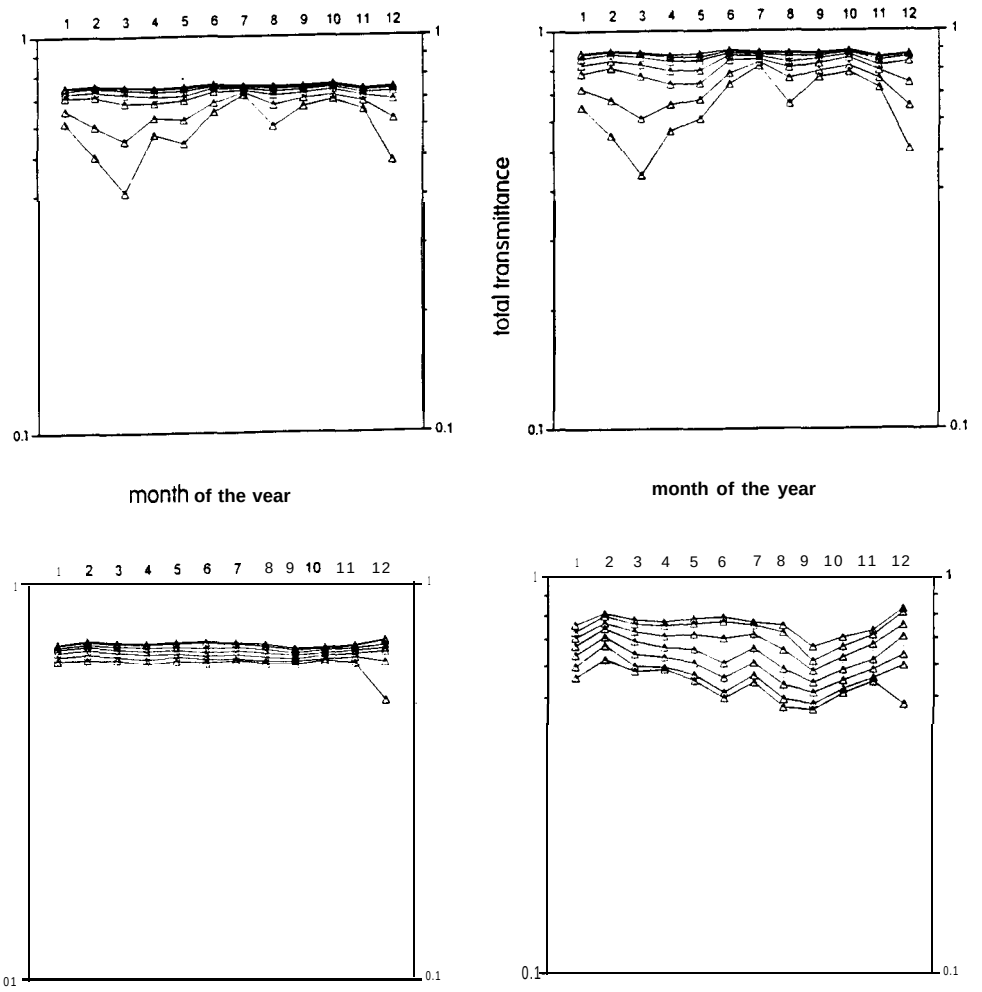

Fig. 5: Cumulative seasonal variation of total transmittance over 1km in the 3-5pm region (left) and the 8-13 µm region (right) at the station Sulayel (top) and Jiddah (bottom). The seven curves represent various n-percentiles with n = 5, 10, 25, 50, 75, 90 and 95, counted from bottom to top.

The conditions in Sulayel are different from those in Jiddah but seem nevertheless more characteristic for desert regions. The 8-13 µm region (for 1 km) is generally 10-15 % "better" than the 3-5 µm region. During the months December to May also larger transmittance reductions can occur. The general form of the curves is mainly determined by the molecular contribution, whereas the aerosol contribution is generally very small. It turned out that only for comparatively short periods the aerosol extinction becomes the dominating factor. This holds for all desert stations, where these events are mainly attributed to sand / dust storms.

4.4 **Estimation of Thermal Ranges Statistics**

The knowledge of range statistics for modern thermal imagers operating under arid climatic conditions is extremely important. On the basis of the meteorological data set described above an estimate of such statistics was performed.

Mathematically the range R of a thermal imager is determined by the intersection point of its $MNTD$ (Minimum Necessary Temperature Difference) and the Effective Temperature Difference (ETD) *[4]*. Both functions are - besides others - a function of range R. The ETD *is* scaled by the absolute value of the initial target-to-background temperature difference, ΔT_0. Thus the following equation has to be solved to calculate a thermal range R of a certain imager and for a certain observation task:

$$ETD = \Delta T_0 \,.\, \tau_{eff}\,(R) = N \,.\, MNTD\,(R)\,, \qquad (1)$$

where $\tau_{eff}(R)$ is the effective, i. e. systems weighted, atmospheric transmittance. N is a normalizing factor converting the $MNTD$ measured under laboratory conditions to real meteorological conditions. The calculations were performed for the following conditions:

thermal imager:	generic system **8-13 pm,**
observation task:	50% recognition probability,
target size:	2.3 m x 2.3 m.

The $MNTD$ was taken from the FGAN-FfO Thermal Range Model (TRM) *[4]*. The effective atmospheric transmittance was calculated via the SYTRAN-Code [1]. The initial temperature difference was estimated from a simple zero order model assuming a sinusoidal diurnal variation of ΔT_0, with a maximum around early afternoon and a minimum during night or early morning hours, both extremes depending on season and cloud cover. Extreme values of AT_o range from 3.5 K (summer, afternoon) to 0.4 K (winter, night and early morning hours).

Equation (1) was solved numerically to obtain the thermal range R for a given meteorological condition. A statistical evaluation is given in Fig. 6, where cumulative frequencies of thermal ranges are plotted for the nine Middle East weather stations and the conditions listed above.

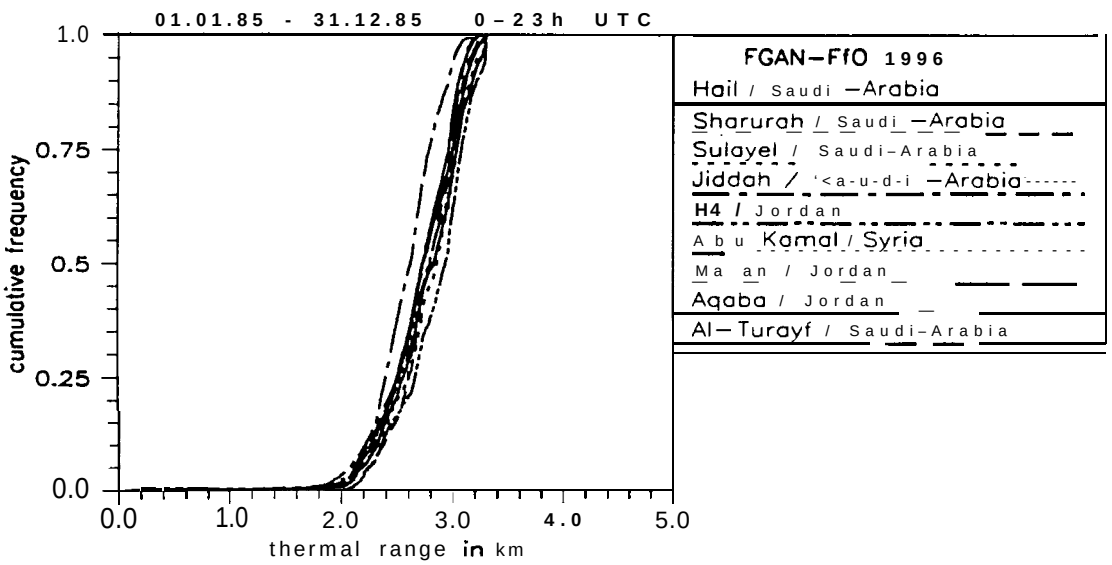

Fig. 6: Cumulative frequencies of tank recognition ranges for a generic thermal imager in the 8-13 µm region at nine Middle East weather stations.

5. Conclusions

Synoptic weather data from nine Middle East meteorological stations have been analyzed with respect to ir propagation conditions. Apart from coastal stations the ir transmittances behave . quite similar at all stations. The conditions at the coastal stations are mainly influenced by high atmospheric water vapor amounts which drastically influences the molecular transmittance contribution.

Statistics of visual ranges cannot be explained by the LOWTRAN 7 Desert Aerosol Model. Therefore comprehensive field measurements on a regular basis performed under desert conditions including aerosol measurements seem extremely necessary to derive well established statistics and a more sophisticated desert type aerosol model.

The individual characteristics of ir propagation conditions at each station will certainly be influenced also by local climatological and orographic effects. A detailed interpretation of the results will, however, only be possible, when related information will be available.

To derive realistic thermal imager performance ranges, additional relevant target-background models have to be established and the influence of clutter to be included, which can be quite excessive under desert conditions.

References

[1] Halavee, U., W. Jessen, A. Hirneth, A. Kohnle: Systems-Weighted Infrared Broad-Band Atmospheric HorizontalTransmittance: The Computer Code SYTRAN, Report FGAN-FfO 1981/78

[2] Kneizys, F. X., E.P. Shettle, L.W. Abreu, J.H. Chetwynd, G.P. Anderson, W.O. Gallery, J.E.A. Selby, S.A. Clough: Users Guide to LOWTRAN7, AFGL-TR-88-0177, ERP No. 1010, August 1988

[3] Longtin, D. R., E.P. Shettle, J.R. Hummel, J. D. Price: A Wind Dependent Desert Aerosol Model: Radiative Properties, AFGL-TR-88-0112, April 1988

[4] Büchtemann, W., D. H. Höhn, W. Wittenstein: Thermisches Reichweitenmodell des FGAN-FfO, Report FGAN-FfO 1977/23

Acknowledgements

The authors are grateful to the German Weather Service, Seewetteramt Hamburg, for providing the basic data set.

Our thanks are also due to Hans-Jörg Neu, who helped us analyzing the data and preparing the graphical presentations.